

CERN Report

ATLAS ITk

Hunter Sharron

Summer 2023

Supervised By Richard Teuscher & William Trischuk



McMaster
University



INSTITUTE OF
PARTICLE
PHYSICS



Contents

1	Introduction	2
2	Endcap Module Thermal Cycling	2
2.1	R3_020 Thermal Cycling Data analysis	4
2.2	R3_021 Thermal Cycling Data Analysis	5
2.3	R3_022 Thermal Cycling Data Analysis	6
3	ASIC Readout Threshold	10
3.1	Introduction	10
3.2	Threshold S-Curve Fits	10
3.3	Threshold Distribution in the ASIC	12
4	Higgs to Four Leptons Decay Plots	14
4.1	Background	14
4.2	Higgs Decay Plots	15
5	Conclusion	16

1. Introduction

My name is Hunter Sharron, currently a fourth year honours physics student studying at McMaster University in Hamilton Ontario. The first half of my summer was spent working with the ATLAS ITk group at the University of Toronto working on endcap module readouts for the high luminosity LHC upgrade. Then the second half of my summer was at CERN funded through the IPP summer student fellowship, where my work involved plotting some ASIC threshold readouts and Higgs to four leptons decay plots.

2. Endcap Module Thermal Cycling

Firstly we shall discuss the motivation behind this project: CERN is currently planning a high luminosity upgrade of the LHC (Large Hadron Collider). With this upgrade ATLAS will also be upgrading its detector, with the purpose of replacing the old detector as it is reaching the end of its lifetime. This new detector shall take advantage of recent advancements in technology and overall improve the previous design; the detector will have an improved radiation tolerance to deal with the increased radiation from the higher luminosity. ATLAS ITk (ATLAS Inner Tracker) is the inner most layer of the ATLAS detector: the inner tracker is comprised of two sections, the endcap modules and the barrel modules. These two sections can be seen in Figure 1, with the barrel modules acting as cylindrical layers wrapped around the collision point and the endcap modules acting as "lids" to the barrel. The term module refers to the individual silicon detector "building blocks" that combined make up the detector. In this report all data analysis was done on endcap modules, so the term endcap will be dropped and all modules should henceforth be assumed to be endcap modules. Another term of relevance is a hybrid; this refers to the circuit placed on top of the silicon and is used to house the ABC Star and HCC (Hybrid Control Chip) Star chips. The ABC Star chips obtain the readout from each strip on the module and sends it to the HCC Star where it is outputted to the Petal. The Petal which is shown in Figure 2, will house all six end cap modules; combined with other Petals it will form a disk that will make up each layer of the endcap detector. The petal hosts the R0 module as its inner most layer and R5 module as its outermost radial layer. Each module contains a power board with a DC-DC converter, that prevents overloading power to the chips and allows the module to function as designed.

Currently the University of Toronto is thermally cycling R0 and R3 endcap modules, which have two and four hybrids respectively; these modules are cycled with a coldbox which can be seen in Figure 3. Each coldbox is equipped with four Peltier cells and thus is capable of thermal cycling up to four modules simultaneously. The Peltier cells are used to raise the temperature up to $+40^{\circ}\text{C}$ and lower it to -35°C . This though is the old temperature range that was used during all data acquisition in this paper, ATLAS ITk recently updated the thermal cycling temperature range to $+20^{\circ}\text{C}$ and -35°C . This was done for two main reasons: firstly the LHC will only raise its temperature once a year to room temperature for maintenance and otherwise will remain at a constant -20°C during operation. Secondly, the larger temperature range

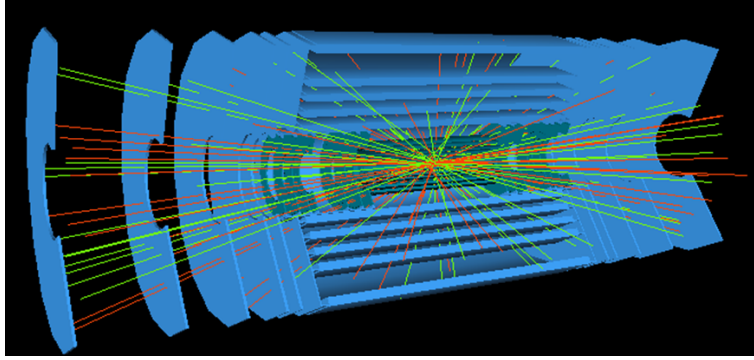


Figure 1: ATLAS Detector Inner Tracker

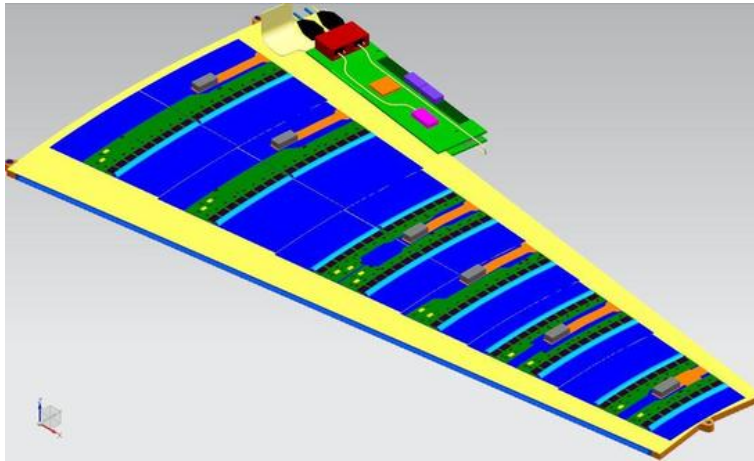


Figure 2: A Fully Assembled Petal With all Endcap Modules

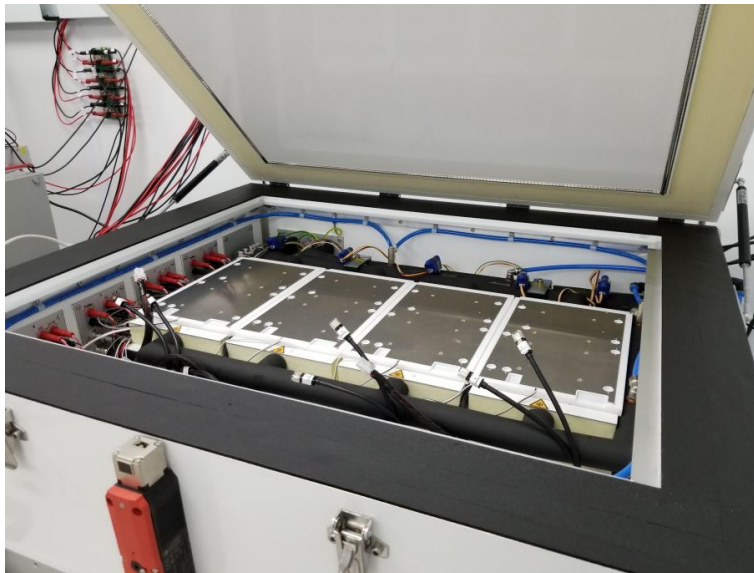


Figure 3: Inside the University of Toronto's Coldbox

was increasing the rate of module failure and modules were beginning to break under conditions they would never realistically be under.

Continuing on with some more preliminary terminology, the terms stream 0 and

stream 1 will be used frequently throughout this chapter. The channels of the module are comprised of two distinct classes, stream 0 and stream 1. The difference is that stream 1 channels are covered by a hybrid and possibly a power board directly above the silicon channel; this could interfere with the channel, causing our readout to be susceptible to extra noise from the hybrids or power board. These two streams are shown in a sample R3 in Figure 4, with the Stream 0 in the "away" section and the Stream 1 in the "under" section of the figure. The finally term of relevance is a Shunted cycle; this term is used to define a cycle accompanied a higher voltage applied across the readout. This cycle is normally done cold, but in rare instances is taken at room temperature. It should be noted though that the ATLAS collaboration has since halted all Shunted cycles as it had a high correlation with module failure. For the purposes of this report at the time of data acquisition these higher voltage cycles were still being performed.

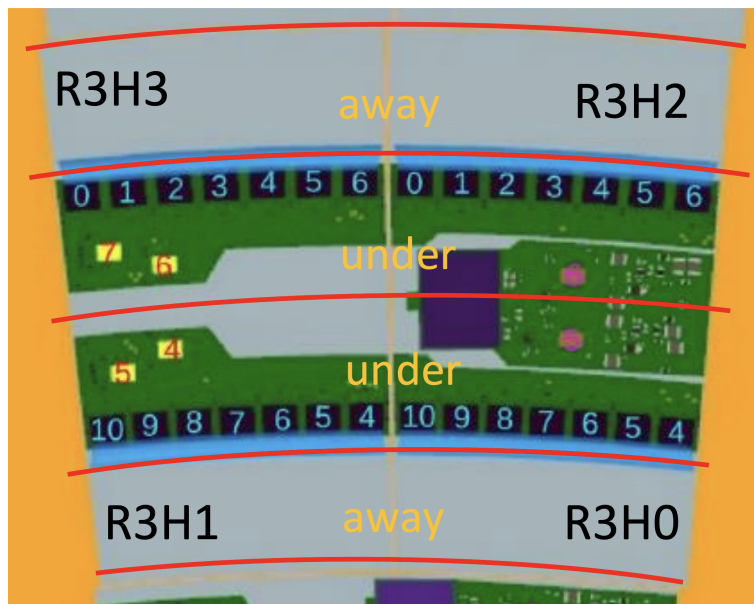


Figure 4: A sample R3 endcap module showing the four hybrids. The black squares are the ABCStar chips and are located on the green circuits, which are the hybrids. The power board is between hybrid 2 and hybrid 0. The yellow squares are the HCCStar chips. The sections labeled "away" are the Stream 0 channels and the "under" are the Stream 1 channels.

2.1 R3_020 Thermal Cycling Data analysis

In the beginning of the summer an R3 module with serial number 020 was thermally cycled by the University of Toronto's coldbox. This module was simultaneously thermally cycled with another R3 module with serial number 021;x as we will see in the next section this created a high correlation between the two data sets. The R3_020 module had a total of 24 cycles each with a readout scan, 11 hot, 11 cold and 2 room temperature scans; three quantities were measured for each strip, the noise, the vt50 cutoff, and the gain. The noise is measure of the background "noise" in a given channel; there are several electric components on the module, each contributing to the noise in a

channel. This quantity is of great importance as if the noise is too high then our signal may be hidden by the noise in the channel, so harder to detect. The vt50 cutoff is the voltage threshold of a channel; this is the highest voltage that can be applied across a readout before a channel stops outputting anything, and this quantity will be given a more formal definition in the next chapter. The gain tells us at what rate the threshold takes effect and is mathematically defined as the derivative of the readout with respect to the voltage; this will be elaborated on in the section on threshold readout S-curves.

One of the data analysis tools used were correlation matrices for each hybrid and stream of the module. These matrices displayed how correlated a cycle scan is with the other cycles; a correlation number is in the range $[-1, 1]$ and is given by the formula,

$$C_{xy} = \frac{\langle (x-\mu_x)(y-\mu_y) \rangle}{\sigma_x \sigma_y}.$$

Where σ denotes the standard deviation, $\langle \rangle$ is the average of all channels, and μ is the mean of the data set. A $C = 1$ means the two sets are totally correlated, while the opposite $C = -1$ refers to total anti-correlation. If $|C| \geq 0.7$ the two sets are strongly correlated; $0.5 \leq |C| \leq 0.7$ shows moderate correlation; $0.3 \leq |C| \leq 0.5$ is a weak correlation; for $|C| \leq 0.3$ the two sets have little to no correlation and can be considered independent. Each square contains the correlation number for the two cycles that comprise the row and column of the matrix element. The color of each matrix element is used to visualize the correlation, with darker blue/purple squares representing high correlation relative to the mean correlation between the cycles, and lighter blue showing lower correlation relative to the average correlation number.

The correlation matrix for stream 0 of hybrid 2 is shown in Figure 5. A distinct pattern is clearly shown by the groups of dark purple squares. This is easily explained once it is considered that cycle 3, 5, 9, 11, 15, and 17 or each purple matrix element, are all cold shunted cycles. If we recall a cold shunted cycle is one where a higher voltage is applied across the readout during a cold temperature scan. What this correlation matrix is telling us, is that the higher voltage has a noticeable effect on our module. So much so, that each shunted cycle is clearly differentiable from a non shunted cycle. This is to be expected as applying a higher voltage across any circuit will in most cases make a distinguishable difference; the higher voltage scan is designed to create stress on the module and observe the effects. The pattern is mutually exclusive to hybrid 2 and does not appear in any correlation matrix of the other hybrids. This means that the higher voltage affected hybrid 2 noticeably more than the other hybrids. It should be noted that the stream 0 correlation matrix was chosen over the stream 1 due to the correlation pattern being significantly more defined in the stream 0 correlation matrix. This is likely due to the increased noise in stream 1 from proximity to module components.

2.2 R3_021 Thermal Cycling Data Analysis

The module R3_021 was thermally cycled simultaneously with the previously discussed R3_020 module. As mentioned before during a scan three quantities are measured: the gain, the vt50 cutoff and the average noise of the given channel. Something of notoriety from this data analysis can be seen when plotting only the hot temperature cycles. This is the clear spike in gain and vt50 in stream 0 of hybrid 3 during the

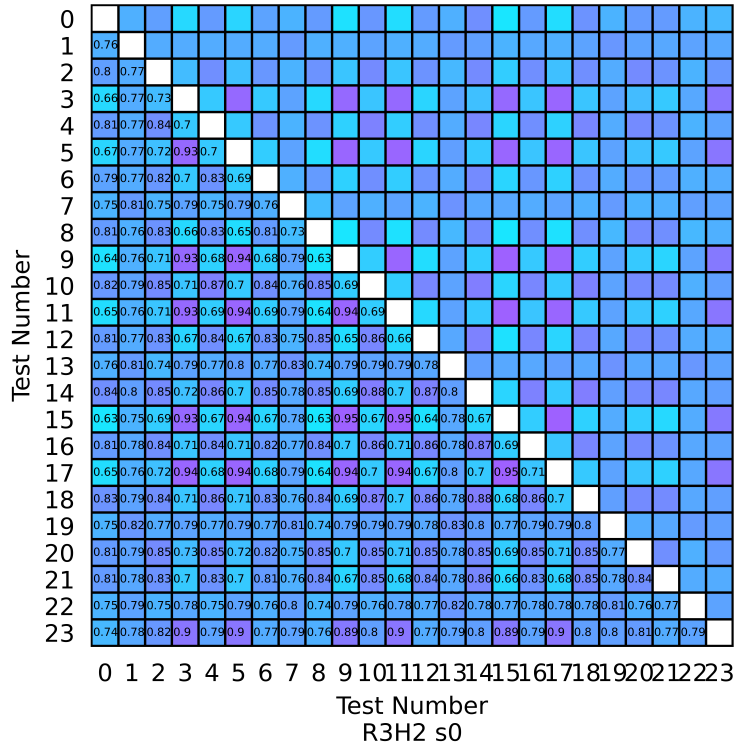


Figure 5: R3.020 Hybrid 2 Stream 0 Correlation Matrix.

5th hot cycle, shown in Figure 6, although strangely the noise is left unfazed. Both of these spikes have managed to pass the outlier filter put in place. This filter removes any outlier not within 4σ , meaning that 3 out the outlier channels nearest 4 neighbours are also outlier channels.

Looking directly at the scan during the 5th cycle, the outlier is clearly located on channels 887-896 on hybrid 3. This is shown in Figure 7, the columns of numbers in the figure from left to right are, the channel numbers, the error code, the gain, the vt50, the noise, and the output comment. The scan in the lower half of the figure shows 10 malfunctioning channels in a row; this above the tolerance of bad adjacent channels. If this was not a pre-production module it would fail the quality control check and would not make it into the ATLAS experiment. As a cause for the malfunction it can be noted in the previous cycle a shunted cold scan was performed. During this scan approximately the same cluster of channels demonstrated an earlier malfunction, shown in Figure 8. It may be interpreted that the 5th hot cycle was not cause for the malfunction, but rather the previous shunted cold cycle. The higher voltage if recalled is known to apply further stress on the modules module, thus it is possible that this may be the cause for our malfunction. Interestingly, the faulty channels disappeared during the next temperature scan and the group of channels functioned properly for the remainder of the thermal cycle.

2.3 R3_022 Thermal Cycling Data Analysis

The final data analysis performed on an endcap module is that of R3_022. An important note on the thermal cycling of this module, half way through being thermally

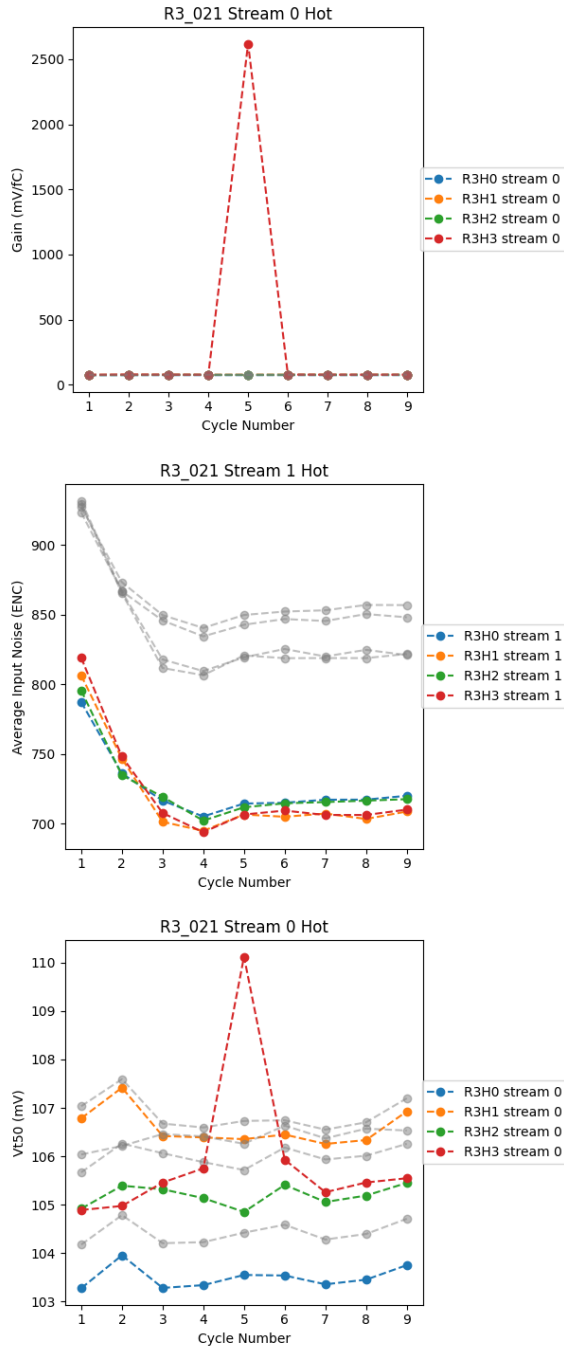


Figure 6: R3_021 Hot Cycle plots in order from top to bottom are, the Stream 0 Average Gain, the Stream 1 Average Noise, and the Stream 0 Average vt50 cutoff. Each colour is a different hybrid, except for the four grey lines, which are the hybrids of the other stream.

cycled two out the four hybrids on the module broke. These hybrids remained broken for the remainder of the thermal cycle and all attempts to revive said modules were unsuccessful. More specifically the hybrids stopped working during the 15th cycle or the 4th shunted cold scan. This can be seen in Figure 9, which shows the 15th cycle where the hybrids died. As can be seen in the figure we were unable to obtain a readout from hybrid number 2 and 0 during the 4th shunted cold scan. It should be noted that

886	0	76.4	104.6	776	OK
887	0	75.1	102.0	769	OK
888	0	77.9	105.1	763	OK
889	0	76.2	105.8	798	OK
890	0	76.6	107.6	810	OK
891	4000	76.1	104.5	992	high noise
892	80000	62.5	103.7	3229	very high noise
893	4	34.9	100.4	20329	inefficient
894	4	2278149.2		4502.2	79 inefficient
895	4	356.9	258.1	13163	inefficient
896	200	84.3	110.5	700	high gain
897	0	78.7	106.7	706	OK
898	0	79.6	109.5	695	OK
899	0	77.7	108.0	700	OK
900	0	78.6	107.4	684	OK
901	0	78.1	106.3	697	OK
884	0	92.5	118.0	724	OK
885	0	94.0	119.8	726	OK
886	0	92.2	117.9	788	OK
887	4000	88.3	113.5	952	high noise
888	4000	87.1	111.3	1514	high noise
889	4	76.4	108.7	2974	inefficient
890	4	64.6	100.7	8665	inefficient
891	4	-54.1	-186.3	0	inefficient
892	4	-50.7	693.3	0	inefficient
893	4	-78.2	589.0	0	inefficient
894	4	-5.5	533.2	0	inefficient
895	4	-22.1	549.8	0	inefficient
896	20000	102.0	126.6	705	very high gain
897	0	93.7	118.0	661	OK
898	0	96.3	121.6	671	OK
899	0	95.3	119.6	649	OK

Figure 7: Two scans performed on Hybrid 3 of R3_021 during the 5th Hot Cycle, showing channels 880-900.

887	0	75.4	105.3	783	OK
888	0	77.4	108.4	803	OK
889	0	76.6	106.2	806	OK
890	4000	76.4	106.9	884	high noise
891	4000	76.5	105.3	1250	high noise
892	4	50.3	94.2	8196	inefficient
893	4	-38.2	54.8	0	inefficient
894	4	520.5	409.6	26022	inefficient
895	4	198.9	221.4	19520	inefficient
896	200	84.3	110.6	704	high gain
897	0	77.9	106.8	710	OK
898	0	80.3	109.6	701	OK
899	0	78.2	108.3	699	OK
900	0	78.9	107.7	700	OK
901	0	78.1	107.0	719	OK
902	0	77.4	106.1	685	OK

Figure 8: The scan performed on Hybrid 3 of R3_021 during the Shunted Cold Cycle directly before the 5th Hot Cycle.

both these hybrids are adjacent to one another and are located on the right half of the module, shown in the sample R3 module in Figure 4.

Checking the correlation matrix for Hybrid 1 in Figure 10, there is a distinct light blue plus pattern in the matrix. More specifically each light blue square is either in row 14 or column 14. This translates to cycle 14 having a significantly lower correlation to other cycles relative to the average correlation among the cycles. This means that the cycle 14 or the 6th hot cycle had noticeably different readout values relative to the other cycles. Since this is the cycle directly previous to cycle 15, the cycle where we saw two hybrids fail, cycle 14 may have been showing early warning signs of hybrid failure and if noticed could have possible saved our two hybrids. Looking at the average noise of cycle 14 relative to the other hot cycles in Figure 11, it can easily be confirmed that yes the readout is noticeably different, by the clear spike in noise during the 6th hot cycle. Another factor of importance that has been previously stated is the high correlation between the higher voltage of a shunted scan and module failure. Cycle 14 might have caused the hybrid failure or was an early warning sign, but it is impossible to know now. However, what can be stated is that the higher voltage applied across the readout during cycle 15 did not help the already slightly malfunctioning hybrids and may have been the tipping point for the hybrids.

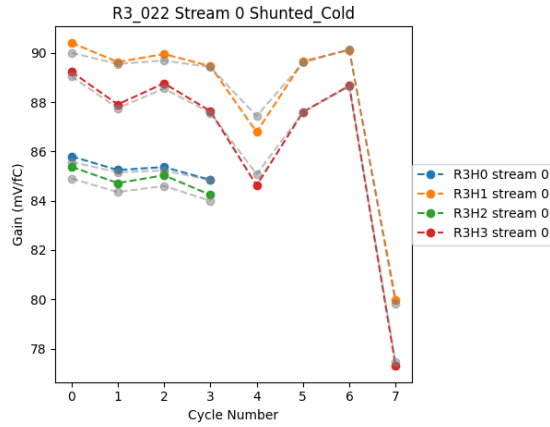


Figure 9: The Gain of the Shunted Cold Cycles performed on R3_022.

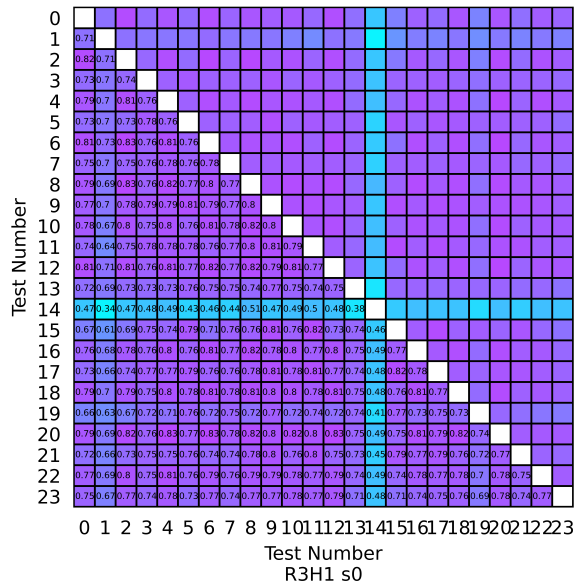


Figure 10: R3_022 Hybrid 1 Stream 0 Correlation Matrix

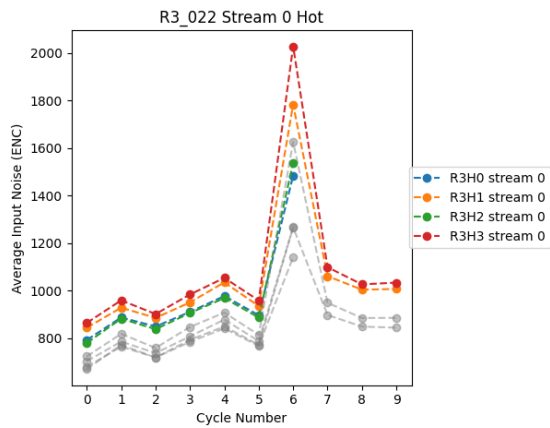


Figure 11: R3_022 Stream 0 Average Noise of Hot Cycles.

3. ASIC Readout Threshold

The following next two chapters include the data analysis performed while at CERN for ATLAS ITk, during the second half of the summer. This work can be broken up into two projects and thus two separate chapters. The motivation behind these two projects was the mastery of ROOT, a data analysis framework developed by CERN; it is widely adopted by the high energy physics community.

3.1 Introduction

To begin, the objective of this project is to extrapolate the readout thresholds for given channels of an ASIC from readout data taken at different voltages. More precisely, each channel is sampled 100 times at each voltage; in each sample we send a count, which acts as a signal sent to the ASIC that is supposed to read out if we are below the threshold. To do this, we set a constant input voltage on the front end of the ASIC and then scan the threshold by varying the threshold setting of the ASIC for each measurement. When the voltage applied across the readout is lower than the readout threshold, the number of counts received from the ASIC is greater than 50. Similarly, if the voltage is greater than the readout threshold the number of counts received is less than 50. It should be clear that the readout threshold is defined as the voltage where 50 counts are received or half of the number of counts sent. The readout threshold is equivalent to the vt50 cutoff mentioned in the previous section. Unless the voltage is near the readout threshold, the number of counts received will normally be 100 counts or 0 counts depending on if the voltage is higher or lower than the readout threshold, this can be seen in Figure 12.

3.2 Threshold S-Curve Fits

When looking at the readout data in Figure 12 we see the readout stays close to 100% efficiently at low voltage and then sharply drops to 0% once surpassing the readout threshold. This data is best fitted by an S-Curve or Sigmoid Function, defined as

$$S(x) = \frac{P_0}{1 + e^{-P_1(x - P_2)}},$$

where P_0, P_1, P_2 are the three fit parameters used to minimize χ^2 . The effectiveness of this fit is shown in Figure 12; in this figure we see a red graph as our fit and the black data points with error bars as the readout data. The fit shown is from channel 752; the same fitting process was applied to all 1280 channels in the ASIC. From the fit we can extract the original desired value, the readout threshold. This is done by noting that a sigmoid function crosses the value 0.5 exactly at P_2 , thus by finding our best fit we also obtain the readout threshold for each channel. A quantity that has been previously mentioned but can now be better explained is the gain. We define the gain as the slope or derivative of the S-Curve at the vt50 cutoff point or at the readout threshold.

The bisection method was next applied to every channel fit with the purpose of extrapolating the minimum number of readout data points needed to create the same fit. The idea behind this is that if we know we only need to do five or six

measurements in the voltage range 40 mV to 75 mV, that is much more efficient than doing 31 measurements in the range 0 mV to 160 mV. This allows us to obtain the same fit and threshold readout, but saves a lot of time. The bisection method can be seen in action in Figure 13, where the bisection method was applied to the fit from Figure 12. The bisection in Figure 13 tells us that when we do future measurements we only need to check the range 40 mV to 75 mV and only perform 5 measurements instead of 31. To apply the bisection method, first two voltages are chosen as the starting points of the bisection, with the only caveat being that they both should be sufficiently far from the readout threshold and the readout threshold must be in between the two voltages. In our case we set $a = 0$ and $b = 160$ as our two starting points, we then find the midpoint between a and b , denoted as c . So $c = \frac{a+b}{2}$, we then plug c into our original S-Curve fit and check if $S(c) < 0.5$ then we set $a = c$ and we add the nearest data point to c to our new bisection plot. Vice versa if $S(c) > 0.5$ then we set $b = c$ and also add the nearest readout data point to c to our new bisection plot. This is then repeated recursively until the data point nearest to the readout threshold is found and added to the bisection plot.

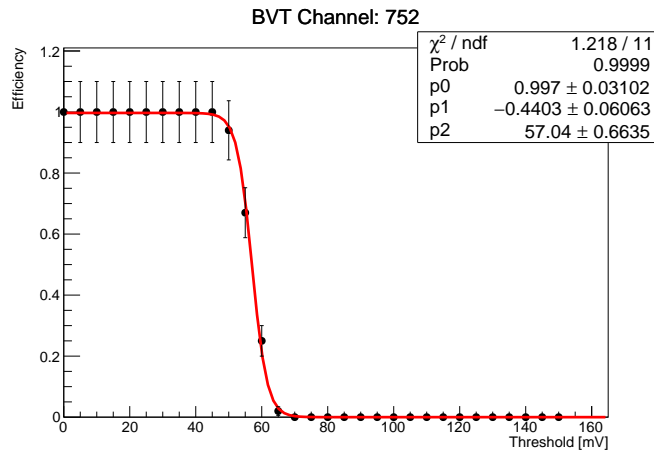


Figure 12: Channel 757 Readout Data, Fitted by a red S-Curve.

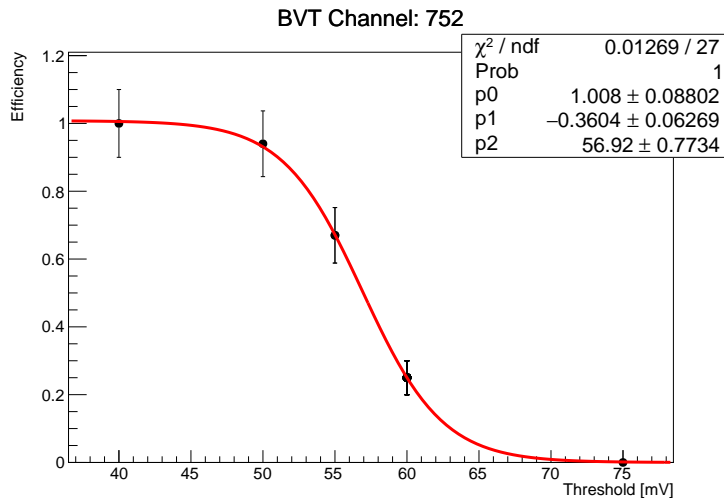


Figure 13: The bisection method applied to the fit for channel 752.

3.3 Threshold Distribution in the ASIC

The next focus point of the project after determining the readout threshold for each channel is looking at the distribution of the threshold. This is first done by looking at the distribution of thresholds on the ASIC, to see if there are clumps of high or low threshold. To do this a heat map was used to visually show the distribution of thresholds along the ASIC. This heat map is shown in Figure 14, colours are used to show the magnitude of the threshold with the lighter yellow channels showing a higher threshold up to 70 mV and the darker blue channels showing a lower threshold down to 40 mV. Figure 14 does not show any clear pattern in the distribution of threshold along the ASIC, with no obvious clumps of high or low threshold near the edges and anywhere along the ASIC. It should be noted that this data is from 2016 and all ASIC problems discussed in this chapter have already been solved by the ATLAS collaboration.

Next we plot a histogram of the number of channels with a given threshold as function of threshold. This can be seen in Figure 15, we expect to a Gaussian like distribution due to the central limit theorem. But instead there are quite a few outlier channels around 60 mV, this is not at all what we expected to see. Not only because we see the histogram is not a nice bell curve, but no threshold should be higher than 60 mV. More specifically a threshold higher than 60 mV is considered unacceptable and is outside the acceptable range of threshold values. Thus if these threshold values are accurate then the ASIC is consider faulty and cannot be used.

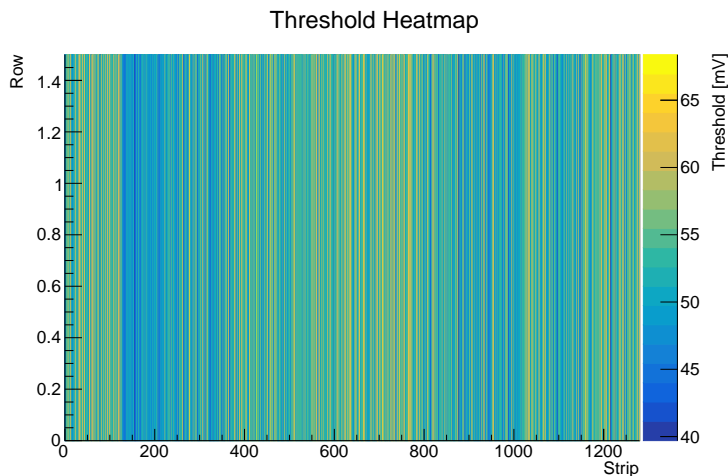


Figure 14: A heat map showing the threshold of each channel along the ASIC. The darker blue channels have a lower threshold and the lighter yellow ones have a higher threshold.

An investigation was then launched into checking these higher threshold channels for a possible source of error in the data analysis or more insight into where they come from. First the data analysis was checked, by looking at the S-Curve fits for higher threshold channels, the accuracy of the fits and thus the threshold may be verified. The S-Curve fits shown in Figure 16 are that of high threshold channels with a threshold greater than 60 mV, the acceptability cutoff threshold for a channel. When looking at the fits in this figure its clear there is no error in the fits, each fit has a relatively small

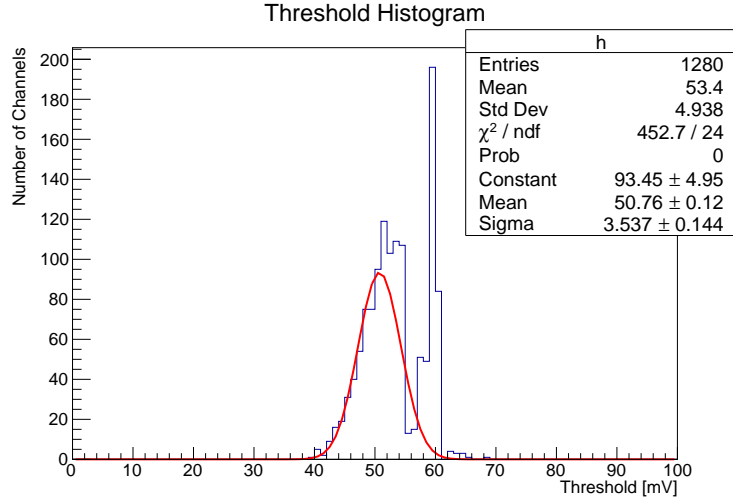


Figure 15: A histogram of the number of channels with each threshold, with the histogram shown in blue and the attempted Gaussian fit shown in red.

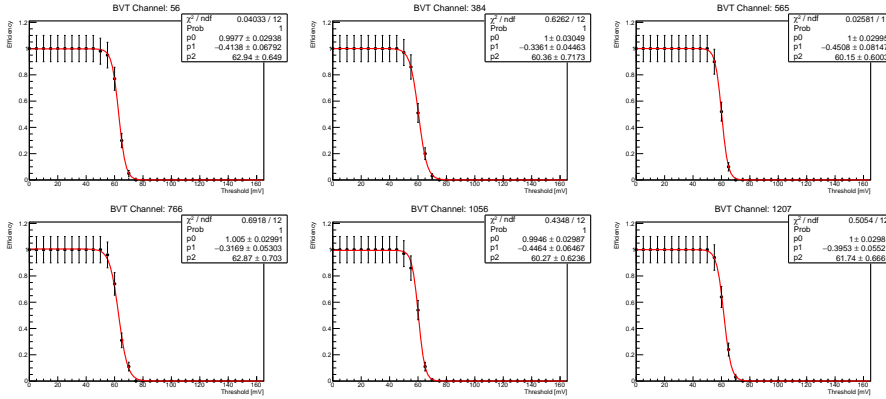


Figure 16: All six figures show the fits for channels with a high threshold, greater than 60 mV.

χ^2 and appears to align with the data points quite well. In addition to the six higher threshold fits shown in Figure 16, all channels with a threshold greater than 60 mV were each checked for errors in the data analysis and no discrepancies were found. This led to checking the distribution of these high threshold channels along the ASIC. Possibly there are clumps of high threshold channels near the edges or center of the ASIC, this would tell us it is a manufacturing problem and that the assembly of the ASIC near the edges or center is causing the faulty channels. A heat map was created to check this, shown in Figure 17. This heat map only contains high threshold channels, so that it visualizes where on the ASIC the high threshold channels are located. Observing the figure it becomes quite clear that there is no pattern in the distribution of these faulty channels along the ASIC. This means that the faulty channels are not caused by poor manufacturing along a certain region of the ASIC. But instead they occur equally as likely anywhere along the ASIC, meaning that poor manufacturing of the whole ASIC is not to blame for just one region. Again it should be stated that this readout data is from an older ASIC in 2016 and does not apply to the current ASICs in development by ATLAS ITk.

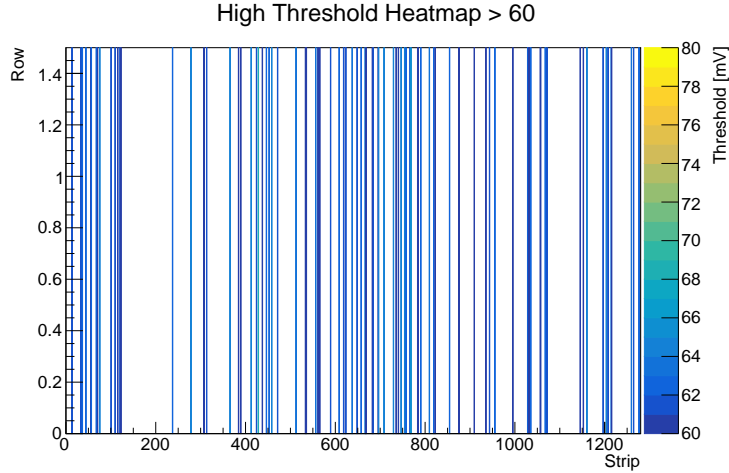


Figure 17: A heat map with only high threshold channels, any channel with a threshold greater than 60 mV.

4. Higgs to Four Leptons Decay Plots

This is the last and final project to be completed during the summer. It is also the smallest of the three projects, with quite limited time to complete relative to the other two projects. The data analysis for this project was done on data from the ATLAS detector in 2016.

4.1 Background

The Higgs boson is arguably currently the most well known fundamental particle, second only to the electron. This is due to its only recent discovery in 2012, making it the most recent fundamental particle to be experimentally verified, and was the last particle missing in the Standard Model that needed to be experimentally verified. Nevertheless, most of the high energy physics community had already accepted the Standard Model, as it was able to make experimental predictions to high precision and explain phenomena that before were a complete mystery.

The Higgs boson is a virtual particle as it normally lives off the mass shell, meaning that it may only exist for small amount of time. This phenomena is due to the Heisenberg uncertainty principle $\Delta E \Delta t \leq \frac{\hbar}{2}$, allowing for a small energy to be created from nothing so long as it only lives for a small lifetime. The Higgs boson is simply an excitation of the Higgs field, a scalar field that exists everywhere in space time. This acts almost as a molasses, in the sense that the field couples to all matter particles and "slows" them down. Without this coupling all matter would be massless and would be traveling at the speed of light c . This is why the photon is both massless and travels at speed c ; it does not couple with the Higgs field.

As mentioned previously, the Higgs has very small lifetime on the order of 10^{-22} seconds. Since it is unstable it decays, one of these decay patterns being the Higgs to four Leptons decay. This pattern can be seen in the Feynman diagram in Figure 18, as

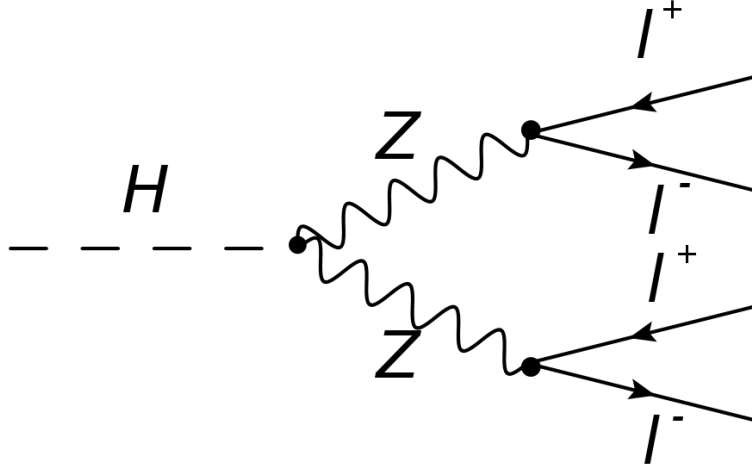


Figure 18: Feynman diagram for Higgs decay to four Leptons.

shown a Higgs boson first decays into two Z bosons, which each decay into two leptons. One of the leptons is the anti matter equivalent of the other, so that charge is conserved in the decay. A lepton is an elementary particle with spin $\frac{1}{2}$, there are three flavours of leptons (electron, muon, tau) and their corresponding neutrino flavours (ν_e, ν_μ, ν_τ).

4.2 Higgs Decay Plots

The first decay plot created is the Higgs to 4 Leptons invariant mass plot, which can be seen in left of Figure 19. In fundamental units mass may be expressed in terms of energy, we choose to express mass in terms of V as it is the most convenient unit to use in high energy physics. In each Higgs decay plot the blue and red stacked histogram each represent the simulated data for the background and Higgs signal respectively. The black data points with error bars are the real measurement taken from the ATLAS detector in 2016. We expect to see a peak in mass around 125 GeV as this is the mass of the Higgs boson, and sure enough there is a distinct peak in both the simulated and real data at 125 GeV. The invariant mass is measured by reconstructing the tracks from the 4 leptons and summing their invariant mass.

The next plot is the Higgs to 4 Leptons transverse momentum plot, this is shown in the right of Figure 19. The transverse momentum is a measure of the momentum of the particle tracks in the transverse plane, this is the plane with normal parallel to the beam axis. The bin width in the figure increases at higher GeV, this was done so that the data would be better visualized. Otherwise there would just be a large steep peak at low energies. Most of the events have a transverse momentum in the range $[0, 45]$ GeV, this is to be expected as most of the colliding particle's momentum is perpendicular to the transverse plane.

Two more Higgs Decay plots are shown in Figure 20, the first of which on the left is a histogram of the number of events as function of the number of jets in that event. A jet occurs when a quark or a gluon hadronizes, the hadron decays into gluons, which decay into other gluons until finally they form stable particles such as protons or Kaons. Most events have either zero or one Jet, more than that is rare but still occurs. This can be seen in Figure 20, with most events only having zero or one jets, and very

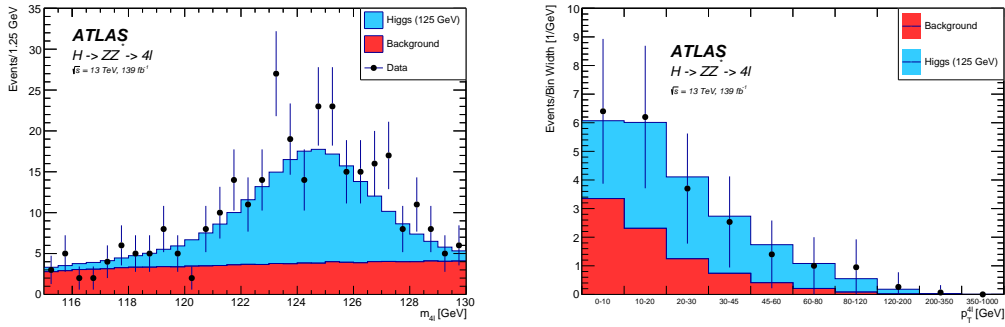


Figure 19: The figure on the left shows the invariant mass plot of the Higgs to 4 Leptons decay channel. The figure on the right shows the plot of the transverse momentum of the Higgs to 4 Leptons decay channel.

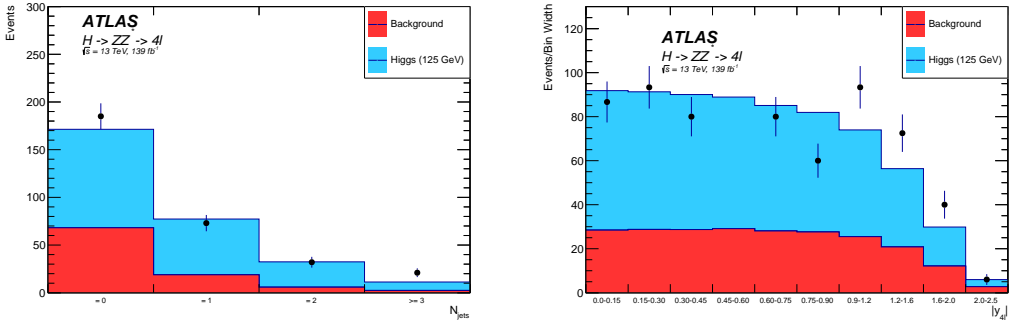


Figure 20: The figure on the left shows the distribution of the number of jets in the Higgs to 4 Leptons decay channel. The figure on the right shows the plot of the rapidity of the Higgs to 4 Leptons decay channel.

few events having 3 or more jets. The figure on the right in Figure 20 is a plot of the rapidity of the Higgs to 4 Leptons decay channel. The rapidity or also sometimes called the pseudo rapidity is a logarithmic measure of angle relative to the beam axis shown in Figure 21. It is defined by $\eta = -\ln(\tan(\frac{\theta}{2}))$, where θ is the angle relative to the beam axis; $\eta = 0$ is parallel to the beam axis and for large values η is perpendicular to the beam axis. In the figure most events occur in the region $0 \leq \eta \leq 1.2$, with few events in the region $1.2 \leq \eta \leq 2.0$ and very few events when $\eta > 2.0$. This is to be expected as most events will stay closer to the beam axis, and few will be found perpendicular to said axis. Also the region $0 \leq \eta \leq 2$ encompasses up to $\theta = 15.14^\circ$ or 74.86° relative to the beam axis, this is 83% of the angular region. So given that most events stay within the beam axis it makes sense that the number of events per bin width decreases as η increases and that most events occur in the region $\eta \leq 2.0$.

5. Conclusion

To conclude, this report was comprised of three different projects each completed over the summer, the first at the University of Toronto and the final two at CERN. First the endcap module data analysis, where correlation matrices and temperature thermal

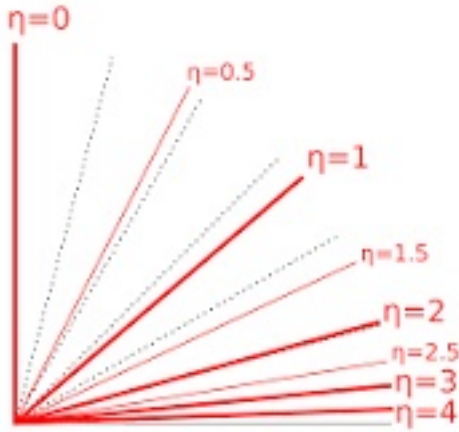


Figure 21: Visual representation of η .

cycling plots were used to extrapolate the meaning of the noise, vt50 and gain data from thermal cycling. The data analysis of the R3_021 module showed a speak in gain and vt50 during the 5th hot cycle. This lead us to find a cluster of channels malfunctioning during the cycle, after further investigation it was found that this cluster actually first appeared during the previous cycle. This previous cycle being a shunted cold cycle, lead us to the conclusion that these channels were most likely damaged by the higher voltage applied during the previous shunted cold cycle. Another interesting case being the data analysis of the module R3_022, where two hybrids died half way through the thermal cycle. After investigating the data, this could have possibly been prevented if the early warning signs the cycle before had been known.

The next project, the ASIC readout threshold, used an S-Curve fit on readout data to determine the readout threshold a channel. Then the minimum number of points needed to create the fit was determined using the bisection method. After plotting the distribution of the threshold it was noted that an alarming number of channels had a high threshold greater than the acceptable tolerance. When these channels were investigated further it was realized that the cause of the high threshold channels was not from an error in the data analysis or from faulty manufacturing along the edges or center of the ASIC. Instead poor manufacturing of the older ASIC design may be to blame, as the faulty channels were located along the whole ASIC and not just one region.

Finally four Higgs to 4 Lepton Decay channel plots were made, the first being an invariant mass plot showing the 125 GeV peak of the Higgs Boson signal. Next a plot was made showing the transverse momentum of the decay channel where most of the transverse momentum lay in the region $[0, 45]$ GeV. Then a histogram was created of the number of events with a given number of jets, where it was noted that most events only have one or zero jets and events with a jet number of three or greater are rare. Lastly a plot of the number of events as a function of rapidity was shown where most of the events occurred close to the beam axis or more precisely when $\eta \leq 2$.

References

- [1] G. Aad et al. “Measurements of the Higgs boson inclusive and differential fiducial cross sections in the 4ℓ decay channel at $\sqrt{s} = 13$ TeV”. In: *The European Physical Journal C* 80.10 (Oct. 2020), p. 942. ISSN: 1434-6052. DOI: [10.1140/epjc/s10052-020-8223-0](https://doi.org/10.1140/epjc/s10052-020-8223-0). URL: <https://doi.org/10.1140/epjc/s10052-020-8223-0>.
- [2] *Technical Design Report for the ATLAS Inner Tracker Strip Detector*. Tech. rep. Geneva: CERN, 2017. URL: <https://cds.cern.ch/record/2257755>.